

Article

Laboratory Evaluation of Alkali-Activated Slag Concrete Pavement Containing Silica fume and Carbon Nanotubes

Abolfazl Mohammadi Janaki^{1,a}, Gholamali Shafabakhsh^{1,b,*}, and Abolfazl Hassani^{2,c}

¹ Faculty of Civil Engineering, Semnan University, Semnan, Iran

² Faculty of Civil Engineering, Tarbiat Modarres University, Tehran, Iran

E-mail: ^amohammadi@semnan.ac.ir, ^bghshafabakhsh@semnan.ac.ir, (Corresponding author),

^chassani@modares.ac.ir

Abstract. Engineers and contractors strive to find the best type of concrete pavement for use in various conditions and applications due to poor performance of asphalt pavements in different climatic conditions, rapid erosion of pavement, poor durability and change in performance characteristics during operation and being non-economic during the period of operation compared to concrete pavements, and not being consistent with the sustainable development principles due to the use of oil-based adhesives. The most common use for portland cement is in the production of concrete that has led to production of greenhouse gases, including carbon dioxide, and global warming has been one of its consequences. More attention has been paid to alkali-activated concrete pavement as a solution because of these effects. The present study has investigated the behavior of alkali-activated slag (AAS) concrete pavement containing silica fume and carbon nanotubes (CNTs). For this purpose, silica fume and CNTs were used as additive for active alkali slag concrete, respectively. The flexural strength, compressive strength, tensile strength, chloride ion charge passed and durability against freeze-thaw cycles was decreased and water penetration was increased by adding silica fume and the use of CNTs in concrete has increased flexural strength, compressive strength, tensile strength, chloride ion charge passed and durability against freeze-thaw cycles and decreased water penetration. The addition of CNTs should have an optimum amount of 5%, so that the mechanical properties and durability of concrete will be decreased by adding more of this additive. The best mix design is for alkali activated slag carbon nanotubes (AASN5) sample, the properties of flexural strength (9%), compressive strength (15%), tensile strength (15%) and chloride ion charge passed (38%) of the AASN5 sample have increased compared to AAS for 28-day curing and penetration (33%) and weight loss decreased after freeze-thaw cycle.

Keywords: Mechanical properties, alkali-activated, concrete pavement, carbon nanotubes.

ENGINEERING JOURNAL Volume 25 Issue 5

Received 6 June 2020

Accepted 12 April 2021

Published 31 May 2021

Online at <https://engj.org/>

DOI:10.4186/ej.2021.25.5.21

1. Introduction

Engineers and contractors strive to find the best type of concrete pavement for use in various conditions and applications due to poor performance of asphalt pavements in different climatic conditions, rapid erosion of pavement, poor durability and change in performance characteristics during operation and being non-economic during the period of operation compared to concrete pavements and not being consistent with the sustainable development principles due to the use of oil-based adhesives. Nowadays, concrete pavement is considered as a reliable option for pavement to construct many of the world's great roads. The most common use for portland cement is in the production of concrete that has led to produce greenhouse gases, including carbon dioxide, and global warming has been one of its consequences. More attention has been paid to alkali-activated concrete pavement as a solution because of these effects [1, 2]. The present world cannot be imagined without concrete and its most important adhesive component, cement. Although there are different concrete types for different applications, the very diverse family of cement types and their properties including durability, fire resistance and low cost, the availability of materials needed for production has made them the most widely used materials used in various industries such as road construction [3].

The geopolymerization is an integrated process for the synthesis of geopolymers which involves the reactions between two parts of raw materials: solid aluminosilicate oxides and alkali metal silicate solutions in a high alkalinity medium resulting in a non-crystalline to semi-crystalline three-dimensional polymer structure, including Si-O-Al bonds, which helps the concrete pavement to have a high durability [4]. Geopolymer is made by activating aluminosilicate with alkaline hydroxide solutions and alkaline silicate and curing at temperatures up to 120°C. The geopolymers have amorphous or nano-sized semi-crystalline structures depending on the curing temperature. The sources of aluminosilicate used in the synthesis of the geopolymers include fly ash, kaolin, metakaolin, metallurgical slag, such as blast furnace slag and aluminosilicate minerals. The activation solutions are usually potassium or sodium silicate sodium or potassium hydroxide can be used with them [5, 6].

People generally expect infrastructures to have longer lifespan and service. Ideally, less money should be spent on road maintenance. Many scientists and engineers seek the best solution to design structures with more durability and guarantee lower repair costs and longer life span. Many costs and damages have been imposed on society due to the low quality and durability of concrete and road structures and its environmental impacts [7]. Nanoparticles are a group of new materials that have been able to enhance the mechanical and physical properties of concrete. Nanomaterials will be able to completely change the concrete world in very

small surfaces due to their properties, its small size can be associated with improving mechanical properties and durability. Nanotechnology has made it possible to produce materials atom-by-atom, therefore using nanotechnology has greatly improved and controlled the physical, mechanical, and durability properties of materials. The microscopic structure and transport of nanoscale materials have a significant effect on the strength and service life of concrete structures [8, 9]. The advancement of nanoscience has made it possible to use them in concrete and the properties of concrete containing these nanomaterials have been investigated. Carbon nanotubes (CNTs) are considered one of these nanomaterials. CNTs are considered one of the best reinforcing agents for composites due to their high diameter (apparent ratio) and high strength. The possibility of improving the cement properties can be expected to prevent cracking by using these materials [10, 11].

CNTs are manufactured in cylindrical form in single-walled and multi-walled form up to several millimeters in length. The mechanical properties of the concrete improve significantly by adding small amounts of these materials to the cementitious material. Increasing the life of concrete pavements is very important and the increase of the durability and mechanical properties can be investigated in two aspects of preventing cracking and repairing cracks if they exist [12]. Deb et al. replaced slag with 0, 10, and 20% fly ash, and used alkaline activating solution at 35 and 40% of the total cementitious material, respectively. The efficiency of geopolymer concrete decreased with increasing slag rate, if other items are unchanged, as well as additional water increased efficiency and decreased strength [13]. Mathew et al. investigated the impact of bottom ash replacement on slag-ash mixtures. According to their results, slag and ash mixtures at high and normal temperatures are able to obtain high strength, but this parameter will be reduced by adding bottom ash [14]. Bagheri and Nazari attempted to investigate the effective factors on the compressive strength of geopolymer concrete containing class C fly ash. Four factors, including slag percentage (30, 50 and 55% as aggregate), curing temperature (25, 70 and 90°C), sodium hydroxide concentration (5, 8 and 12 M) and curing time at this temperature (4, 8 and 16 h), were investigated to evaluate the compressive strength. According to the results, the curing temperature is the most important factor on the compressive strength of the specimens. The second effective factor is the slag percentage [15]. Ramazanipour and Moeini during a study concluded that active alkali paste containing nano silica had higher durability, compressive strength and more chloride ion penetration than active alkali paste [16]. Fakhim et al. during a study added 0.1 to 2% carbon nanotubes, aimed at investigating the microstructure of specimens containing these nanotubes. Tensile strength of specimens containing 0.3% carbon nanotubes showed tensile strength up to 70% more than control specimens and tensile strength decreased by adding the carbon

nanotubes and the tensile strength decreased further with increasing carbon nanotube consumption. According to the results of thermal weighting analysis, the cement hydration was improved in the presence of carbon nanotubes and specimens containing carbon nanotubes showed more strength according to the results of mercury permeation test [17].

Miri et al. during a study investigated the cracking of concrete containing nano-wollastonite additive on the corrosion performance and service time of reinforced concrete structures. The results were discussed in terms of cracking patterns, crack width, rebar weight loss and rebar diameter degradation at different levels of corrosion. According to the results, the service life will be increased by using nano-wollastonite in reinforced concrete beams which is associated with increasing the initial cracking time, decreasing cracking growth speed and rebar mass loss [18].

Shah et al. during a study added multi-walled carbon nanotubes (MWCNTs) to cement and concluded that the use of 0.03 to 0.1 wt.% of MWCNTs led to obtaining the best mechanical properties of cement nanocomposites, further, flexural strength was increased by 8 to 40% and the shrinkage was reduced by 30 to 40% [19]. Zhou et al. investigated the compressive strength of concrete with modified aggregates containing carbon nanotubes at different ages of curing. According to the results, the compressive strength of concrete with modified aggregates containing carbon nanotubes decreased and the ductility increased at different ages of curing [20]. Guan et al. investigated the mechanical properties of concrete containing MWCNTs by weight percentages of 0, 0.05, 0.1 and 0.2 wt%. According to experimental results, MWCNTs play an important role in increasing flexural and compressive strength of concrete, flexural and compressive strength of concrete containing 0.05 wt% of MWCNTs increased by 70% and 25%, respectively [21]. Rocha et al. investigated the mechanical properties of concrete containing carbon nanotubes, they concluded that mechanical properties were improved by increasing the percentage of carbon nanotubes in concrete. With addition of 0.1% carbon nanotubes in cement paste, fracture energy was increased by 90%, flexural strength was increased by 46% and tensile strength was increased by 47% [22].

This research not only helps the environment, Investigates the effect of silica fume and cementitious carbon nanotubes on the mechanical properties and durability of alkali-activated concrete. In recent years, thematic research has been conducted in this field, none of which has comprehensively introduced the use of alkali-activated slag concrete containing silica fume and carbon nanotubes.

2. Lab Program and Materials

2.1. Aggregates

The aggregates presented in Table 1 are used to make active alkali slag concrete specimens according to ASTM C33 [23].

Table 1. Sieve aggregates analysis (mm).

Coarse aggregates	Aggregate size (mm)	25	19	9.5	4.75	2.36
	Percentage of screening sieve(%)	100	96	38	8	0
Fine aggregates	Aggregate size (mm)	1.18	0.6	0.3	0.15	0.075
	Percentage of screening sieve(%)	82	58	26	7	2

2.2. Blast Furnace Slag

Slag is the main binder in the alkali activated slag (AAS) concrete composition. In this study, slag with a specific weight of 2.754 kg/cm³ was used. The chemical composition of the slag used is obtained using the XRF test and is presented in Table 2.

Table 2. Chemical compounds of silica fume and slag.

Chemical composition	Silica fume (wt %)	Slag (wt %)
SiO ₂	90	33.02
CaO	0.97	40.21
Al ₂ O ₃	0.67	9.69
MnO	0.98	1.59
Fe ₂ O ₃	0.22	0.59
Na ₂ O	0.98	0.57
K ₂ O	0.9	0.93
MgO	1.2	7.72
TiO ₂	-	2.12
Ba	-	0.16
SO ₃	-	3.26
P,Cl,Cr,Ni,Rb,Y,Th	3.5	a few

2.3. Silica Fume

In order to improve some of the concrete properties during manufacture, silica fume is added to the concrete. In the present study, silica fume was added as powder to the alkali activated slag (AAS) concrete mixture, chemical compounds of silica fume are listed in Table 2.

2.4. Slag Activator

Mix design has been implemented according to ACI 211/1 standard. Nano clay particles with weight percentages (1%, 2% and 3%) were used in this survey and also a (control) sample without nano clay additive was used in this study. Table 3 shows constituent

elements for design of mixtures. Water-to-cement ratio was considered 0.425 for all specimens.

Table 3. The ingredients of sodium silicate solution.

Chemical Properties	Na ₂ O	SiO ₂	H ₂ O
Weight percentage	8.2	27	64

Table 4. The ingredients of sodium hydroxide.

Chemical Properties	Na ₂ CO ₃	Ni	K ₂ O	Fe	NaOH
Weight percentage	0.43	0.003	0.066	0.003	99

2.5. Water

In the present study, the water used is drinking water that has no additives.

2.6. Carbon nanotubes (CNTs)

Carbon nanotubes (CNTs) are grown using chemical vapor deposition on slag particles, the CNTs have diameter of 20 to 120 nm and are several micrometers in length. The chemical properties of carbon nanotubes are shown in Table 5.

2.7. Mixing Design

The cementitious material of this concrete is made of slag, silica fume, sodium silicate and sodium hydroxide. The activator was selected so that Na₂O was 0.6 total weight of slag and silica fume. In all mixtures, SiO₂/Na₂O ratio was equal to 1. The ratio of water to cement was 0.425. The volumetric mix design using ACI211-02 was used to make the specimens [24]. In the present study, alkali-activated slag (AAS) contains ratios of 10% and 20% of silica fume and carbon nanotubes with 2%, 5% and 10% ratios. The specimens were extracted from the mold 24 hours after the alkali activated concrete specimens were made, and cured in lime water, Table 6 shows the concrete mix design.

Table 5. Chemical Properties of Carbon Nanotubes Using XRF Test

Chemical Properties	Na ₂ O	MgO	Al ₂ O ₃	SiO ₂	P ₂ O ₅	SO ₃	K ₂ O	CaO	TiO ₂	MnO	Fe ₃ O ₃	Sr
Weight percentage	0.274	2.067	3.022	21.393	0.126	1.975	0.85	62.823	0.276	0.249	2.349	0.065

Table 6. Mixing design for AAS concrete (Kg/m³).

Mix design	Coarse aggregates	Fine aggregates	Slag	Silica fume	Water	Sodium silicate	Sodium hydroxide	Carbon nanotubes
AAS ¹	915	885	400	-	157.2	63	16.1	-
AASSi ² 10	915	885	360	40	157.2	63	16.1	-
AASSi20	915	885	320	80	157.2	63	16.1	-
AASN ³ 2	915	885	392	-	157.2	63	16.1	8
AASN5	915	885	380	-	157.2	63	16.1	20
AASN10	915	885	360	-	157.2	63	16.1	40
AASSi10N2	915	885	352.8	39.2	157.2	63	16.1	8
AASSi10N5	915	885	342	38	157.2	63	16.1	20
AASSi10N10	915	885	324	36	157.2	63	16.1	40
AASSi20N2	915	885	313.6	78.4	157.2	63	16.1	8
AASSi20N5	915	885	304	76	157.2	63	16.1	20
AASSi20N10	915	885	288	72	157.2	63	16.1	40

¹ alkali activated slag.

² alkali activated slag/ silica fume.

³ alkali activated slag carbon nanotubes.

3. Testing methods, Results and Discussion

The present study was carried out to investigate the effect of carbon nanotubes and silica fume on the properties of alkali-activated slag.

3.1. Flexural Strength

In the concrete pavement design, the flexural strength is used to consider the fatigue criterion that controls the corrosion cracking of concrete under repeated loading. Flexural strength test specimens were made at $100 \times 100 \times 500$ mm to perform this test in accordance with ASTM C78 standard, and the specimens were placed under Universal Testing Machine (UTM) after 7 and 28 days of curing in limewater to measure the flexural strength [25]. The flexural strength of concrete beams on two simple supports is determined under four-point flexural load according to this standard and the results are expressed as the rupture modulus. Figure 1 shows the test specimens of flexural strength.



Fig. 1. Examples of flexural beam.

It was anticipated that the use of carbon nanotubes leads to improving the adhesion and consequently the flexural strength of alkali-activated concrete, but the effect of silica fume and carbon nanotubes simultaneously on the flexural strength of alkali-activated concrete was not clearly predictable. As shown in Fig. 2, the highest flexural strength is related to 5% carbon nanotube (AASN5) with alkali-activated slag concrete. This sample can withstand higher stress load compared to other specimens, and the lowest flexural strength is related to the alkali-activated slag specimen AASSi20 containing 20% silica fume. In 28-day specimen of AASN5 compared to AAS, 9% increase in flexural strength was observed. Adding silica fume reduces the flexural strength of concrete because it reduces the amount of binder (slag) by adding carbon nanotubes, so the flexural strength of the cross section increased for the

above-mentioned reasons to reach the optimum value and thereafter the flexural strength decreases due to the decrease in stress-resistant surface due to flexure. Crystallization takes place more rapidly by increasing the number of carbon nanotubes, and carbon nanotubes as a supplement to the fine grains in the mixture filling the pores of aggregates and empty spaces and creates a homogeneous and dense concrete. This reduces the cavities and increases the flexural strength due to better bonding of the stone grains with the mortar as well as the aggregate [26]. It should be noted that this increase has an optimum value of about 5% of the carbon nanotubes and the resistance decreases afterwards.

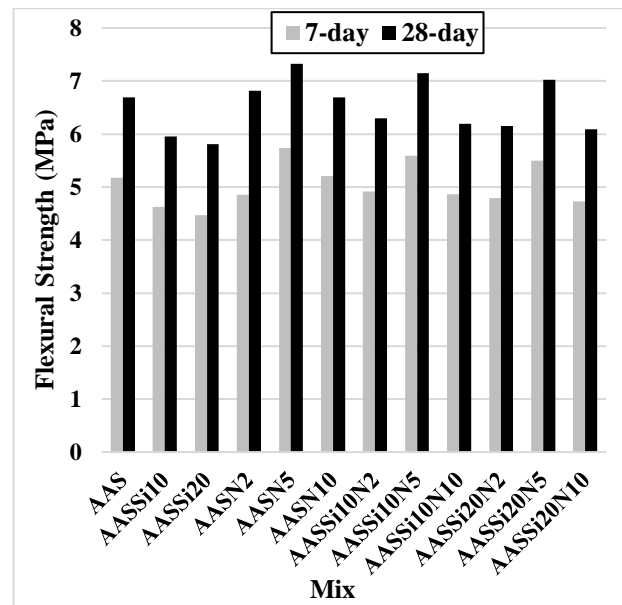


Fig. 2. Comparison of flexural strength of specimens.

3.2. Compressive Strength

The compressive strength test was performed according to ASTM C39. After the cylindrical specimen is placed between the jaws of the compressive strength device, this parameter is equal to the maximum stress that the cylindrical specimen can withstand. According to the standard, the loading rate is considered between 0.14 and 0.34 MPa/s [27]. Compressive strength tests were performed on 7 and 28-day specimens. The results of compressive strength tests on different concrete specimens are shown in Fig. 4. Three replicates of each type of concrete specimen were made to investigate the effect of carbon nanotubes on alkali-activated concrete, the compressive strength of the alkali-activated concrete was reduced by adding silica fume due to decrease in the crystallization speed in alkali-activated concrete by reducing slag content and reducing its 7-day compressive strength. As shown in this Fig. 4, 10% of silica fume has had a significantly better performance than 20% in the specimens. On the other hand, alkali-activated slag (AAS) specimen has a higher strength than specimens containing silica fume. The compressive strength increases by adding carbon nanotubes, the highest 28-day

compressive strength is related to the AASN5 sample (66.2 MPa), which is 15% higher than that of AAS. Therefore, the compressive strength of the section increases for the mentioned reasons to reach the optimal value, and from then on, the amount of compressive strength decreases due to the reduction of the surface resistance to stresses due to the application of pressure.

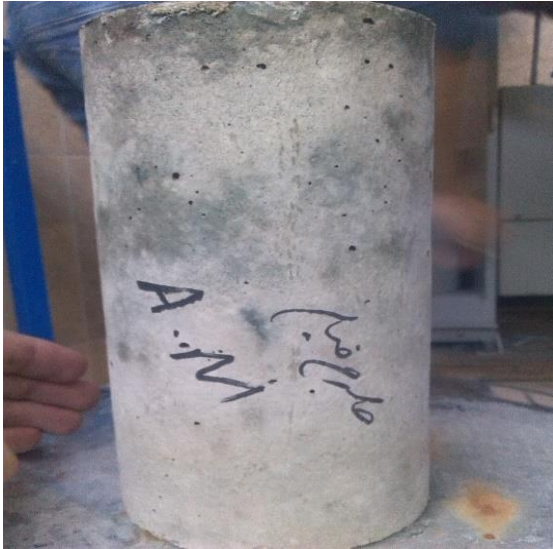


Fig. 3. Compressive specimens.

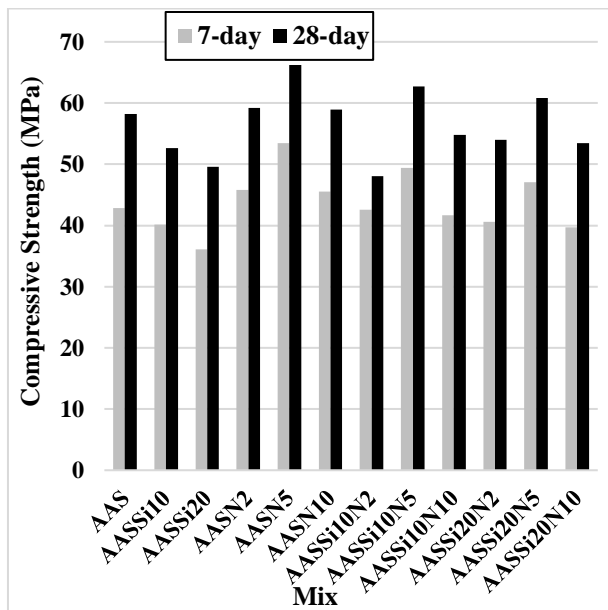


Fig. 4. 7-day and 28-day compressive strength.

3.3. Splitting Tensile Strength

Tensile strength test was carried out on 28-days specimens according to ASTM C496 standard. In this method, 3 replicates were made of each concrete specimen to investigate the effect of carbon nanotubes on alkali-activated concrete, tensile strength test specimens were made in cylindrical dimensions with the diameter of 150 mm and height of 300 mm. 28 days after curing, by applying a diagonal compression force on the

specimen which is placed horizontally between the two test plates, the load was applied continuously, uniformly and without sudden changes with a constant velocity of about 700 to 1400 KPa/min until the concrete ruptures.

The narrow strips of 3-layer plywood strips with a thickness of 3 mm and a width of 25 mm and a length equal to the length of the mold length were used to avoid too high local compressive stresses on the loading lines. These strips should be placed between the specimen and top and bottom pedestals of the test device, or between the specimen and the complementary support plates (if necessary). Support bands should sometimes not be used more than once [28]. As shown in Fig. 5, the activated alkali slag concrete containing 5% AASN5 carbon nanotube (6.48 MPa) has higher tensile strength than other mixtures, the tensile strength is increased in this concrete specimen compared to AAS 15%. In the specimens that silica fume replaced with slag, the tensile strength decreased with increasing silica fume. The tensile strength of the alkali-activated concrete increased by adding carbon nanotubes, it should be noted that this increase has an optimum value of about 5% of the carbon nanotubes and then there is a decrease in strength.

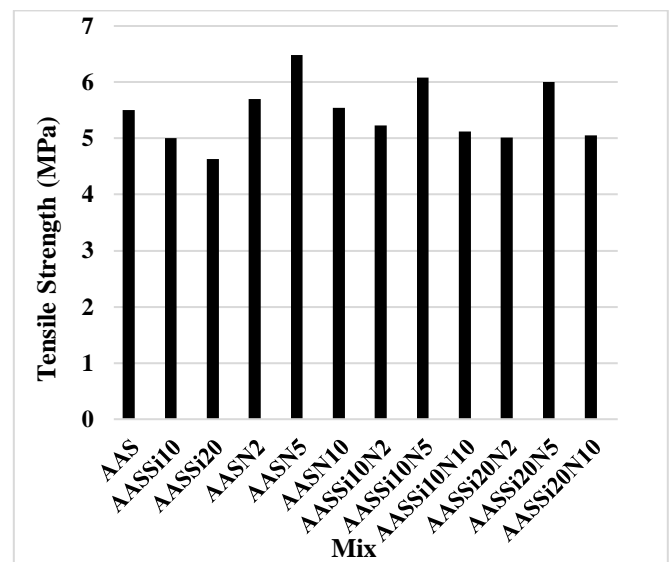


Fig. 5. Tensile strength results.

3.4. Rapid Chloride Penetration Test (RCPT)

According to ASTM-C1202 standard, the test was performed on different mixtures. A cylindrical specimen with diameter of 100 mm and thickness of 50 mm were used in this test. After applying the vacuum and saturating it with water, the specimen was placed inside the apparatus cell, the concrete specimens were exposed to NaCl solution in one direction and NaOH solution in the other. The electrode is connected to the positive pole on one side of the cell where the NaOH solution is located and the electrode on the other side of the cell where there is salt solution, is connected to the negative pole of the direct current generating device and the voltage is applied at 60 V through electrodes. The charge

passed is recorded within 6 hours. By calculating the area under the time current curve, the electric charge passing through each sample (electric flux) is calculated at the age of 28 days. In fact, this method measures the amount of electrical charge passing through the concrete sample during the test time as chloride penetration index [29]. According to the results of the rapid chloride penetration test (RCPT) test, as shown in Fig. 6, the highest charge passed is related to AASN5 (6100 Coulombs) and the lowest belongs to AASSi20 (3759 Coulombs). An increase in the charge passed the concrete is observed in the AASN5 concrete sample by 38% compared to the AAS sample. According to the results, there is a significant decrease in the chloride ion penetration in the AASN5 sample and in fact an increase in the charge passed. Finally, it was concluded that the passing current increased by increasing the carbon nanotubes, and the charge passed decreased with increasing silica fume.

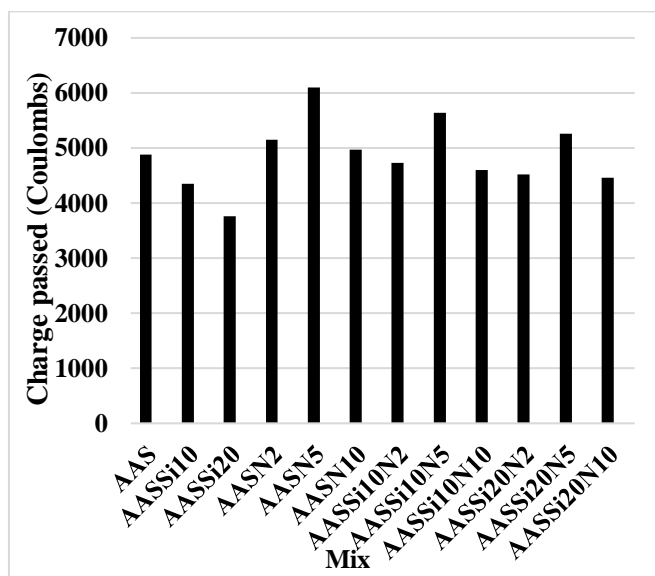


Fig. 6. The charge passed through concrete.

3.5. Water Penetration in Concrete

The concrete structure has a significant impact on concrete penetration and material transfer rate through concrete. It is necessary to determine the concrete penetration coefficient of a structure that the concrete penetration coefficient is the amount of liquid or gas charge passed through the unit of time through the cross-sectional area, under a single hydraulic gradient, in which liquid leakage coefficient is generally used to determine the penetration of concrete, it is determined by the gas or water penetration factors with a contractual index. One of the most important properties of concrete in relation to concrete durability is concrete penetration, which provides the facility for water or other fluids to flow through the concrete and carry harmful materials with themselves into the concrete. Concrete penetration was tested using water penetration test in the concrete according to EN 12390-8 standard. The concrete specimens were made according to the standard with dimensions of 200 × 200 × 120 mm. The concrete

specimens were incubated for 24 hours at 100°C after 28 days of curing, and then placed at 24 ± 2 until it reaches ambient temperature. The specimens were then subjected to permeation apparatus and Bar 5 pressure was applied to the specimens for 72 hours. Then, Brazilian test was used for splitting the specimen into two halves and the maximum water penetration depth was measured [30]. The depth of water penetration test is shown in Fig. 7.

The trend of penetration changes is shown in Fig. 8. According to the results, water penetration of alkali-activated concrete increased by adding silica fume, and the water penetration depth decreased by increasing carbon nanotubes, this water penetration depth decrease has optimal amount that is 5% of carbon nanostructures and the depth of water penetration increases with further increase of carbon nanotube. AASN5 (16 mm) had the lowest water penetration and the highest water penetration was related to AASSi20 (31 mm). A 50% decrease in water penetration was observed in AAS in AASN5 concrete specimen N5 concrete sample compared to AASN5. A 33% decrease in water penetration was observed compared to AASN5.



Fig. 7. Depth of water penetration test in concrete.

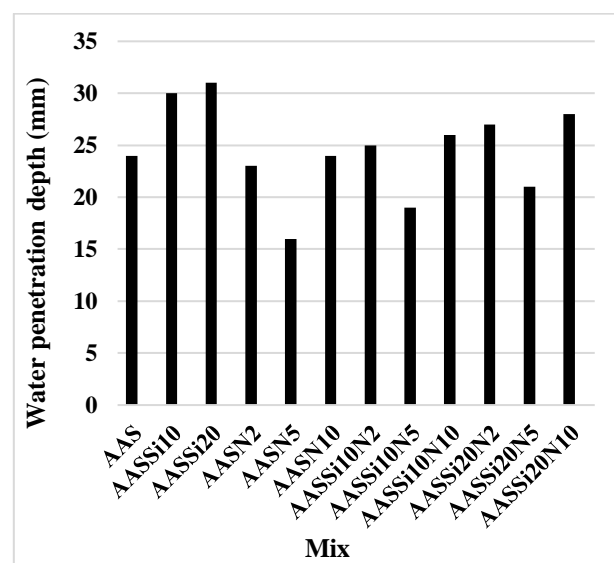


Fig. 8. Depth of water penetration in concrete.

3.6. Freeze-Thaw Cycle Testing

The durability test against freeze-thaw cycling was performed in the form of freezing and sequential flooding and weight loss control according to ASTM C666-A. In the present study, the specimens tested were placed in the freeze-thaw cycling device according to the above standard with dimensions of 78 × 78 × 370 mm and were exposed to 300 temperature cycles between +4.4 to -17.8°C, the samples were removed from the machine after each 36 cycles, their weight loss calculated and their water replaced. This process continued until the specimens experienced 300 cycles, and the weight loss was again measured in the 300 cycles [31]. The freeze-thaw cycling device is shown in Fig. 9. This test was performed to evaluate the effect of silica fume and carbon nanotubes on the durability of alkali-activated slag (AAS) concrete against freeze-thaw cycling. As shown in Fig. 10, the weight loss of concrete increased by increasing the silica fume and the weight loss of concrete decreased as the carbon nanotubes increased, this decrease in weight loss had an optimum value of about 5% of carbon nanostructures and the weight loss of alkali-activated concrete increases with a further increase in carbon nanotube. The lowest weight loss and highest durability to freeze-thaw cycling occurred in the AASN5 concrete specimen, and the highest depth of weight loss was related to the AASSi20 specimen, which had the lowest durability against freeze-thaw cycling and had the highest weight change.



Fig. 9. Measuring the weight of specimens.

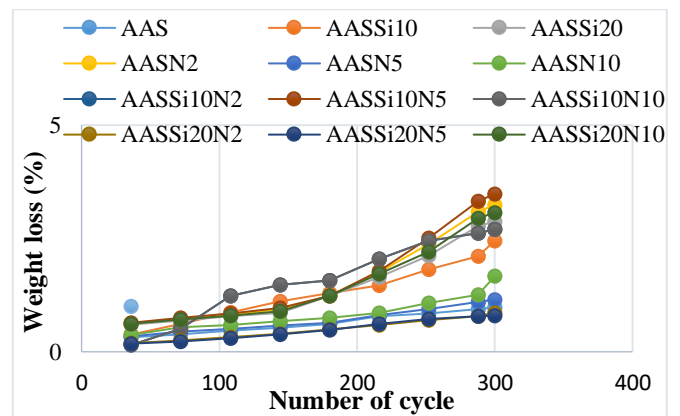


Fig. 10. Cumulative percentage weight loss.

3.7. Relationships

A linear relationship was observed between the results of the flexural strength test and the charge passed of chloride ion through the concrete and the compressive strength test and water permeation depth (Figs. 11 and 12). There is a linear correlation between the flexural strength and the charge pass of chloride ion through the concrete in the concrete with a regression coefficient of 0.91. According to this correlation, there is a direct relationship between the flexural strength and the charge passed, i.e., the charge passed increases with increasing flexural strength. Also, there is a linear correlation between compressive strength and the depth of water penetration with a regression coefficient of 0.77. This linear correlation indicates that there is an inverse relationship between compressive strength and the depth of water penetration, i.e., the depth of water penetration decreases as compressive strength increases.

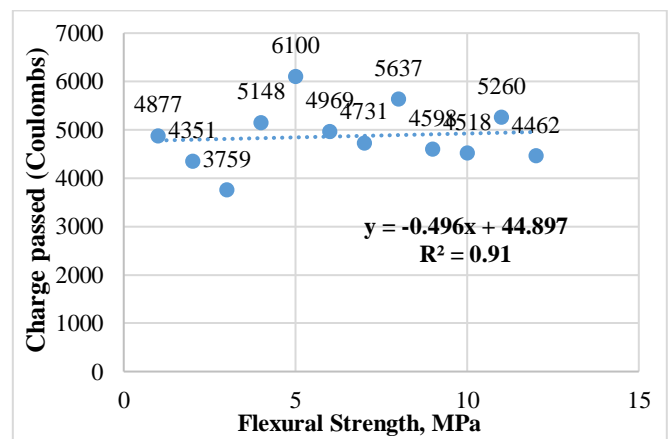


Fig. 11. Relationship between flexural strength and the charge passed of chloride in concrete.

4. Conclusions

In the present study, the mechanical properties and durability of alkali-activated concrete pavement containing silica fume and carbon nanotubes were investigated. For this purpose, silica fume and carbon nanotubes were added as an additive to alkali-activated

concrete, respectively. The following results were obtained in the present study.

1. Mechanical properties and durability of AAS concrete increased by using cementitious carbon nanostructures.
2. The compressive strength, flexural strength, tensile strength, chloride ion charge passed by increasing the silica fume in alkali-activated slag concrete, and freeze-thaw cycle decreased and water penetration increased.
3. The compressive strength, flexural strength, tensile strength, chloride ion charge passed and the durability against freeze-thaw cycle increased by increasing carbon nanotubes in concrete, and water penetration decreased. It should be noted that this increase in carbon nanotubes has an optimum amount of about 5% of carbon nanostructures, and then the mechanical properties and durability of concrete decrease.
4. The best mixing design is related to the AASN5 sample, the properties of flexural strength (9%), compressive strength (15%), tensile strength (15%) and chloride ion charge passed (38%) of the AASN5 sample have increased compared to AAS for 28-day curing and penetration (33%), weight loss after freeze- thaw cycle has decreased.
5. All alkali-activated slag concrete samples containing carbon nanotubes have higher compressive strength, flexural strength, tensile strength, chloride ion charge passed, and durability against freeze-thaw cycle and lower water penetration compared to the AAS sample.
6. A linear correlation is observed between the flexural strength and the chloride charge passed in the concrete. That is, with increasing flexural strength, the chloride charge passed in concrete decreases.
7. According to the results of this study, the use of carbon nanotubes is consistent with the engineering approach and has a rational approach to improving the properties of alkali-activated concrete.

References

- [1] A. Hosan, F. U. A. Shaikh, and M. Alansari, "Influence of nano-CaCO₃ addition on the compressive strength and microstructure of high volume slag and high volume slag-fly ash blended pastes," *Journal of Building Engineering*, vol. 18, no. 1, pp. 1009-1029, 2020.
- [2] P. Gomathi and A. Sivakumar, "Performance evaluation of alkali activated fly ash lightweight aggregates," *Engineering Journal*, vol. 25, no. 5, pp. 77-85, 2013.
- [3] M. S. Imbabi, C. Carrigan, and S. Mckenna, "Trends and developments in green cement and concrete technology," *Journal of Sustainable Built Environment*, vol. 1, no. 5, pp. 194-216, 2012.
- [4] G. Siyao, L. Yu, W. Xiaomei, W. Fei, Z. W. Tiejun, and S. Chen, "Preparation, characterization of highly dispersed reduced graphene oxide/epoxy resin and its application in alkali-activated slag composites," *Journal of Cement and Concrete Composites*, vol. 105, no. 136, pp. 429-438, 2020.
- [5] R. Bajpai, K. Choudhary, A. Srivastava, K. S. Sangwan, and M. Singh, "Environmental impact assessment of fly ash and silica fume based geopolymer concrete," *Journal of Cleaner Production*, vol. 254, pp. 120-147, 2020.
- [6] F. Shahrajabian and K. Behfarnia, "The effects of nano particles on freeze and thaw resistance of alkali-activated slag concrete," *Journal of Construction and Building Materials*, vol. 176, pp. 172-178, 2018.
- [7] M. Luo, C. X. Qian, and R. Y. Li, "Factors affecting crack repairing capacity of bacteria-based self-healing concrete," *Journal of Construction and Building Materials*, vol. 87, pp. 1-7, 2015.
- [8] N. Salemi and K. Behfarnia, "Effect of nano-particles on durability of fiber-reinforced concrete pavement," *Journal of Construction and Building Materials*, vol. 48, pp. 934-941, 2013.
- [9] A. Jamshidi, K. Kurumisawa, G. White, J. Jize, and T. Nawa, "Use of nanotechnology in concrete pavements," *Journal of Composites Part B: Engineering*, vol. 185, no. 2, pp. 383-401, 2020.
- [10] R. Siddique and A. Mehta, "Effect of carbon nanotubes on properties of cement mortars," *Journal of Construction and Building Materials*, vol. 50, pp. 155-171, 2014.
- [11] S. San, "In situ growth of carbon nanotubes/carbon nanofibers on cement/mineral admixture particles: A review," *Journal of Construction and Building Materials*, vol. 49, pp. 835-840, 2013.
- [12] F. H. Ghasan, W. S. Kwok, and R. M. S. Abdul, "Sustainability of nanomaterials based self-healing concrete: An all-inclusive insight," *Journal of Construction and Building Materials*, vol. 23, pp. 155-171, 2019.
- [13] P. S. Deb, P. Nath, and P. K. Sarker, "The effects of ground granulated blast-furnace slag blending with fly ash and activator content on the workability and strength properties of geopolymer concrete cured at ambient temperature," *Journal of Materials and Design*, vol. 62, pp. 32-39, 2014.
- [14] M. B. J. Mathew, M. M. Sudhakar, and D. C. Natarajan, "Strength economic and sustainability characteristics of coal ash-GGBS based geopolymer concrete," *Journal of Computational Engineering Research*, vol. 3, no. 1, pp. 207-212, 2013.
- [15] A. Bagheri and A. Nazari, "Compressive strength of high strength class C fly ash-based geopolymers with reactive granulated blast furnace slag aggregates designed by Taguchi Method," *Journal of Materials and Design*, vol. 54, pp. 483-490, 2014.
- [16] A. A. Ramezani-pour, M. A. Moeni, and P. L. Pratt, "Mechanical and durability properties of alkali activated slag coating mortars containing nanosilica

- and silica fume,” *Journal of Construction and Building Materials*, vol. 163, pp. 611-621, 2018.
- [17] B. Fakhim, A. Hassani, A. Rashidi, and P. Ghodousi, “Preparation and microstructural properties study on cement composites reinforced with multi-walled carbon nanotubes,” *Journal of Composite Materials*, vol. 49, no. 1, pp. 85-98, 2013.
- [18] M. Miri, M. R. Ghasemi, and H. Beheshti nezhad, “Experimental investigation of corrosion cracking in reinforced concrete beams containing nano wollastonite,” *Journal of Rehabilitation in Civil Engineering*, vol. 7, no. 3, pp. 117-138, 2019.
- [19] S. P. Shah, M. S. Konsta-Gdoutos, and Z. S. Metaxa, “Highly-dispersed carbon nanotubes reinforced cement-based material,” United States Patent Application Publication, 0229494A1.
- [20] A. Zhou, R. Qin, and D. Lau, “Effect of carbon nanotubes treated aggregates on compressive strength of concrete,” *Journal of Composites Part B: Engineering*, vol. 25, pp. 15-21, 2020.
- [21] X. Guan, S. Bai, and J. Ou, “Mechanical properties and microstructure of multi-walled carbon nanotube-reinforced cementitious composites under the early-age freezing conditions,” *Journal of Construction and Building Materials*, vol. 233, p. 117317, 2020.
- [22] V. V. Rocha, P. Ludvig, F. D. A. Silva, and A. C. C. Trindade, “The influence of carbon nanotubes on the fracture energy, flexural and tensile behavior of cement based composites,” *Journal of Composite Materials*, vol. 209, pp. 1-8, 2019.
- [23] *Standard Specification for Concrete Aggregates, American Standards for Testing and Materials*, ASTM C33, West Conshocken, 2003.
- [24] *Standard Practice for Selecting Proportions for Normal, Heavyweight, and Mass Concrete*, ACI 211.1-91, ACI Committee 211, 2002.
- [25] *Standard Test Method for Flexural Strength of Concrete (Using Simple Beam with Third-Point Loading)*, ASTM C78, American Society for Testing and Materials, West Conshocken, 2016.
- [26] Gh. Shafabakhsh, A. Mohammadi Janaki, and O. Jafari Ani, “Laboratory investigation on durability of nano clay modified concrete pavement,” *Engineering Journal*, vol. 24, no. 3, pp. 35-44, 2020.
- [27] *Standard Test Method for Compressive Strength of Cylindrical Concrete Specimens*, ASTM C39-18, West Conshocken, 2018.
- [28] *Standard Test Method for Splitting Tensile Strength of Cylindrical Concrete Specimens*, ASTM C496-17, 2017.
- [29] *Standard Test Method for Electrical Indication of Concrete's Ability to Resist Chloride Ion Penetration*, ASTM C1202-18, West Conshocken, 2018.
- [30] *Standard Testing Hardened Concrete, Depth of Penetration of Water Under Pressure*, EN, DIN. 12390-3, 2009.
- [31] *Standard Test Method for Resistance of Concrete to Rapid Freezing and thawing*, ASTM C666, Philadelphia, Pa: Annul Book of ASTM Standards, 2015.





Abolfazl Mohammadi Janaki was born in 1994, Iran. He received his B.Eng. in civil engineering in 2016 from Shahrekord University, Iran, and his M.Eng. in civil engineering in 2018 from the University of Tarbiat Modares, Iran. From 2018, He continues pursuing a Ph.D. degree in civil engineering at the University of Semnan. Her research interests include road and airport pavement, concrete technology, and road construction, and he is currently a lecturer at several universities.



Gholamali Shafabakhsh was born in 1963, Iran. He received his B.Eng. in civil engineering in 1982 from Iran University of science and technology, Iran, and his M.Eng. in civil engineering in 1991 from the University of INSA, French. and D.Eng. in civil engineering from the University of INSA, French, in 1999. Her work includes 120 articles in ISI and ISC journals and 160 articles in domestic and foreign conferences, 5 books in the field of roads and railways, and 4 patents. Her favorite research fields are road pavement, airport, railway engineering and traffic, and she is currently a faculty member with the rank of professor at Semnan University.



Abolfazl Hassani was born in 1955, Iran. He received his B.Eng. in civil engineering in 1981 from Safford University, England, and his M.Eng. in civil engineering in 1986 from the University of Birmingham, England. and D.Eng. in civil engineering from the University of Westminster, England, in 1992. Her work includes 130 articles in ISI and ISC journals and 145 articles in domestic and foreign conferences, 10 books in the field of roads and railways, and 4 patents. Her favorite research fields are road pavement, Concrete, airport, railway engineering and traffic, and she is currently a faculty member with the rank of professor at Tarbiat Modares University.